An Enhanced Dynamic Model for McKibben Pneumatic Muscle Actuators

Ruiyi Tang, **Dikai Liu**
Centre for Autonomous Systems,
Faculty of Engineering and Information Technology,
University of Technology, **Sydney**, **Australia**
Ruiyi.tang@student.uts.edu.au, **Dikai.liu@uts.edu.au**

Abstract

An enhanced dynamic force model of a type of small and soft McKibben-type pneumatic muscle (PM) actuator has been developed. This model takes the factor of external loads and a more sophisticated form of friction into account, and is presented as a polynomial function of pressure, contraction length, contraction velocity and external load. The coefficients in this model are determined from a series of experiments with constant loads and step pressure inputs. Comparison study with other models is conducted assuming the Coulomb friction as a constant force. The results demonstrate a solid enhancement of the presented model.

1 Introduction

The McKibben-type pneumatic muscle (PM) actuator was first introduced by [Gaylord, 1958]. As illustrated in Figure 1, it consists of an inner expandable rubber tube covered by an outer braided mesh sheath. Compared to conventional actuators, the PM actuator has the advantages of high a power-to-weight ratio, inherent safety, low cost and light weight. It has been applied in many robotic researches, such as the exoskeleton robots in [Kang et al. 2009] and [Kobayashi and Suzuki, 2005].

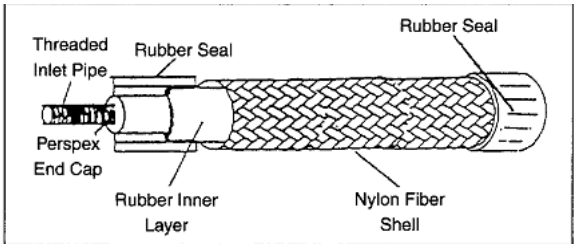

Figure 1: Structure of the pneumatic muscle ([Caldwell et al. 1995])

The drawbacks of the PM actuator are its nonlinear force-length performance, comparatively long response time and the hysteresis effect that is difficult to estimate. Numerous literatures have worked on developing a proper dynamic force model for the PM actuator.

The quasi-static model for the PM actuator can be regarded as an essential part of the dynamic model. It describes the nonlinear relationship between the PM's length $L(t)$ or contraction length $x(t)$, inner pressure $P(t)$, and the contracting force $F(x, P)$. This nonlinear relationship can be derived from the virtual work principle as demonstrated in [Chou and Hannaford, 1996] are shown in as Equation (1):

$$-F(t)dL(t) = P'(t)dV(t) \quad (1)$$

in which $F(t)$, $dL(t)$, $P'(t)$ and $dV(t)$ stand for the contraction force, length change, pressure and volume change, respectively. The left side of the equation represents the output work and the right side represents the input work.

Based on this theoretical model, researchers developed empirical amendments to improve its validity. [Colbrunn, et al. 2001] introduced a correction factor that is related to the inner pressure in order to make the practical static force a certain proportion of the calculated theoretical actuation force. In [Tondu and Lopez, 2000], some parameters that took into account the non-cylindrical shape on the two ends are suggested to have improved the force model. In recent studies, the quasi-static force model was assumed as a simple polynomial function of length $L(t)$ (or contraction length $x(t)$) and pressure $P(t)$ [Petrovic, 2002], [Pujana-arrese et al. 2007], [Wickramatunge and Leephakpreeda, 2009] and [Itto and Kogiso, 2011]. By recording the force, length and pressure values in multiple experiments, the coefficients in the polynomials were empirically determined. For different PM actuators, the coefficients or correction factor in these models may vary. Except for the model in [Wickramatunge & Leephakpreeda, 2009], the other models all suggest a linear relationship between variable $P(t)$ (pressure) and $F(x, P)$ (force). This fact is in accordance with the theoretical derivation in Equation (1).

Dynamic models have been developed based on the static force model by adding friction force elements. Several literatures (e.g. [Chou & Hannaford, 1996], [Colbrunn et al. 2001]) suggested that friction force in the PM actuator consists of a Coulomb friction element and a viscous damping element. It is demonstrated in [Chou and Hannaford, 1996] that the Coulomb friction is the domi-

nant friction force of the total friction of the PM actuator.

Coulomb friction is attributed to the dry friction between the rubber tube and the nylon braided sleeve, as well as the nylon threads' friction between each of the nylon threads ([Yeh et al. 2010]). It is believed that this friction causes hysteresis in the PM actuator's response, which is known as the gap of tension response between the excitation process and the relaxation process, in the experiment of applying the same constant pressure on the PM actuator in [Chou and Hannaford, 1996]. The hysteresis response is related to multiple parameters (e.g. pressure, load, working duration, braided sleeve, diameter and material) and is difficult to be characterised with an accurate mathematical model [Fei et al. 2011]. In some quasi-static force models of PM actuators that include Coulomb friction, the expressions of Coulomb friction are all simplified to some extent. [Chou and Hannaford, 1996] suggested that a simple constant force of *±2.5 N* (positive for extending, negative for contracting) be added to the static force model to count for the effect of Coulomb friction when simplicity is acceptable. [Kang et al. 2009] also regarded Coulomb friction as a constant. In [Colbrunn et al. 2001], the case where the soft PM actuator was tested and oscillated displacement response was obtained, Coulomb friction was modelled as the product of a constant coefficient and the PM actuator's stiffness. The simulation result based on this model did not completely coincide with the experimental results. In summary, we found all these simplified models insufficient to characterise the responses of soft PM actuators used in this research.

In some recent research papers discussing the model based control approaches for PM actuators [Huang et al. 2004] and [Fei et al. 2011], the excitation and relaxation processes are modelled as two separate high order polynomial functions of pressure and contraction length, or characterised by the Maxwell-Slip model. Furthermore researchers in [Balasubramanian et al. 2006] and [Fei et al. 2011] found that external loads on the PM actuators can affect Coulomb friction. In the former paper, Balasubramanian et al. considered the effect of external load when explaining varied frequency and damping ratio of the displacement response in their experiment with constant weight and step pressure input. However, in both studies, the relationship between external loads and Coulomb friction are only quantitatively plotted, and no exact model is presented.

It is also noticed that, in most of the studies, researchers used large PM actuators with diameters over *10 mm*. These PM actuators have higher stiffness when pressured. Given comparatively stiff PM actuators that have large volumes and regulated input air flow rate, the recorded PM actuator responses in the experiments mentioned above (usually displacement responses) can be estimated by simple PM models. For instance, in the study in [Reynolds et al. 2003], the researchers developed an empirical dynamic force model and successfully used it to predict and control the response of a stiff PM actuator.

A more complicated displacement response (with more and larger oscillations in response) of the PM actuator was recorded in [Colbrunn et al. 2001] where a PM actuator with a small diameter (*6 mm*) was pressured with constant air mass, loaded with constant weight on its free end and applied with an initial displacement. Although the developed dynamic force model was complex because of a nonlinear quasi-static force element, a viscous friction element and a non-constant Coulomb friction element, it is still insufficient to accurately estimate the actual complete response of the PM actuator in this case, in spite of the fact that "the natural frequency of estimated and actual displacement response was in good agreement" [Colbrunn et al. 2001].

Therefore, this paper aims to develop a dynamic force model for small and soft PM actuators that is capable of estimating the response more accurately. To achieve this goal, the factor of external loads is taken into account, and a more sophisticated Coulomb friction model is used. Section 2 presents the polynomial function of the developed model, and Section 3 discusses the method of obtaining the coefficients in the model and analysis of the simulation results.

2 Dynamic Force Model

We firstly study the elements that are friction irrelevant, which are the spring force, contractile force, and adjustment force elements. These elements make the static model. According to [Chou and Hannaford, 1996], based on the virtual work principle, the following equation is derived to characterise the static force of a PM actuator:

$$\begin{aligned} F_{static-chou} &= P(t)\frac{3(L_0 - x(t))^2 - b^2}{4\pi n^2} \\ &= P(t)\frac{3x^2(t) - 6L_0 x(t) + (3L_0{}^2 - b^2)}{4\pi n^2} \end{aligned} \tag{2}$$

Where $P(t)$ stands for the pressure inside the PM actuator, n is the thread turns of the outer mesh; b is the thread total length of the outer mesh of a particular PM actuator; $L(t)$ denotes the length of a PM actuator, and L_0 is the nominal length (preloaded resting length) of the PM actuator. Contraction length $x(t) = L_0 - L(t)$.

Based on this, a nonlinear correction force element, F_{adjust}, to account for the error caused by the thickness of the shell and the bladder [Chou and Hannaford, 1996] is introduced. This element can be in different forms, for example, in [Pujana-arrese et al. 2007] it is a fourth order polynomial function. But in this paper, it is assumed as a second order polynomial function of variable $x(t)$ as in Equation (3), because with fewer coefficients it has a simpler form and is found still sufficient to provide accurate force estimation in later experiments. According to Equation (2), the static model is written as:

$$\begin{aligned} F_{static}(x,P) &= K(x,P)x(t) + F_{ce}(P) + F_{adjust}(x) \\ &= \left(K_1 x^2(t) + K_2 x(t) + C_1\right)P(t) \\ &\quad + S_1 x^2(t) + S_2 x(t) + S_3 \end{aligned} \tag{3}$$

Where S_1, S_2, S_3, K_1, K_2 and C_1 are regarded as coefficients and can be determined by the steady-state displacement and pressure responses obtained from step pressure input experiments in the next section.

This research regards the static force model as a special case of the dynamic model in which the friction force in the dynamic model is assumed to be zero. According to the review in Section 1, we propose a dynamic force model as:

$$F(x,P) = F_{static}(x,P) + F_{Damp} + F_{coulomb} \tag{4}$$

in which, Coulomb friction $F_{coulomb}$ is velocity-irrelevant

and viscous damping F_{Damp} is dependent on velocity. Their modelling is discussed respectively.

As was discussed in the last section, a comprehensive Coulomb friction model parameterised by pressure, load, working duration and etc. is necessary for an accurate dynamic model. It is firstly modelled as the dry friction force on the contact surface between the mesh threads and the rubber tube (as in Equation (5)), which is regarded as the cause of Coulomb friction ([Yeh et al. 2010]). Based on the definition of Coulomb friction in [Pytel et al. 2010], it is expressed as the product of the normal force applied on the contact surface of the rubber tube $F_{surface\text{-}Normal}$ and the friction coefficient μ, written as:

$$\begin{aligned} F_{Coulomb} &= F_{Surface-Normal}(P(t), L(t)) \cdot \mu = P(t) \cdot \pi D(t) L(t) \cdot \mu \\ &= P(t)\mu \frac{\sqrt{b^2 - L^2(t)}}{n} L \\ &= \frac{P(t)\mu}{n} \sqrt{b^2 - (L_0 - x(t))^2}\,(L_0 - x(t)) \end{aligned} \tag{5}$$

in which the friction coefficient μ is assumed to be constant. $D(t)$ is the diameter of the cylinder shaped PM actuator, and $D(t)L(t)$ denotes the approximate area of the contacting surface.

The above equation can be approximated as a second order polynomial function of the actuator contraction length $x(t)$:

$$F_{Coulomb}(x, P) = P(t)\left(N_2 x^2(t) + N_1 x(t) + N_0\right) \tag{6}$$

Here, N_0, N_1 and N_2 are the coefficients to be determined. It is also stated in previous literature reviews that, the hysteresis effect caused by Coulomb friction in the PM actuator is related to the loads (in this case the hanging weight) applied on the PM actuator [Balasubramanian et al. 2006]. Considering the effect of external loads on the PM actuator, we add a correction term $\varphi(F_{ext})$ to the above equation, as in Equation (7). In later experiments, $\varphi(F_{ext})$ is empirically approximated to be $\varphi(F_{ext}) = -m$ in the constant weight hanging situation.

$$F_{Coulomb}(x, P) = (P(t) + \varphi(F_{ex}t)) \cdot (N_2 x^2(t) + N_1 x(t) + N_0) \tag{7}$$

For the viscous damping element, on the one hand, the viscous damping was stated to be not as significant as the Coulomb friction and in most existing models it is simplified as the product of a constant damping coefficient and the contraction velocity. On the other hand, according to the analysis in [Colbrunn et al. 2001], that "the damping may not be a constant"; therefore a more sophisticated model for the viscous damping element is developed to ensure the accuracy of the dynamic model. The viscous damping element characterises the viscosity of the compressed air, and the friction between the air and the tube's inner surface. The first part of viscous friction results from the viscosity of the compressed air itself, which is the friction between gas particles in the air. According to [Houghton and Carpenter, 2003], the expression is shown in Equation (8).

The second part of viscous damping is from the skin friction between the compressed air and the inner wall of the PM actuator's rubber tube. Its expression in Equation (8) is based on [McCormick, 1995].

To conclude, the viscous friction between the air particles is nonlinearly related to the average flow velocity $v(t)$, and is modelled as:

$$\begin{aligned} F_{Damp} &= F_{Drag} + F_{viscosity} \\ &= Area \times \mu_{Air} \frac{\partial v(t)}{\partial y} + C_d \frac{\rho v^2(t)}{2} \times Area \\ &= D_1 P \dot{x}^2(t) + D_2 P \dot{x}(t) \end{aligned} \tag{8}$$

in which μ_{Air} denotes the viscosity of air gas, and $v(t)$ denotes the shear velocity. Assuming it is inside a simple round tube; the shear velocity is linearly related to the distance of the air particle to the inner wall of the tube [Houghton & Carpenter, 2003], thus the shear velocity is related to the average velocity $v(t)$. The assumption that contraction velocity of the PM actuator $\dot{x}(t)$ equals the air transmission velocity $v(t)$ is made, similar to that in [Reynolds et al. 2003] and [Breteler et al, 1999]. D_1 and D_2 are the coefficients to be determined by experimental results.

In summary, the dynamic contraction force is expressed as:

$$\begin{aligned} F(x, P) = &\left(K_1 x^2(t) + K_2 x(t) + C_1\right) P(t) + S_1 x^2(t) + S_2 x(t) + S_3 \\ &- P(t)(D_1 \dot{x}^2(t) + D_2 \dot{x}(t)) + (P(t) + \varphi(F_{ext})) \cdot \begin{cases} -\left(N_2 x^2(t) + N_1 x(t) + N_0\right)(\dot{x} > 0) \\ +\left(N_2 x^2(t) + N_1 x(t) + N_0\right)(\dot{x} < 0) \end{cases} \end{aligned} \tag{9}$$

Different from other polynomial-based PM actuator models, this model takes the parameters of contraction length, pressure and external loads into account in developing a more sophisticated form of Coulomb friction to improve accuracy.

3 Experiments

A series of experiments are conducted to obtain the coefficients (K_1, K_2, C_1, S_1, S_2, S_3, N_1, N_2, D_1, D_2) of the dynamic model in Equation (9). The Shadow Robot Company© manufactured PM actuator *Φ6-300 mm* is used in the experiments.

3.1 Test Rig and Experimental Method

As a common approach, similar to the experiments in [Pujana-arrese et al. 2007], [Wickramatunge and Leephakpreeda, 2009] and [Itto and Kogiso, 2011], a series of constant hanging weight and step pressure input experiments were conducted. In each test, a constant load is hung on the free end of the PM actuator and a step pressure is applied to the PM actuator. This is different from the method of using motors to apply the load (force) change on the PM actuator and maintaining constant pressure. In this way, the impact of the insufficiently modelled elements is more evident and the transient response is measured. The experimental setup is shown in the following figure.

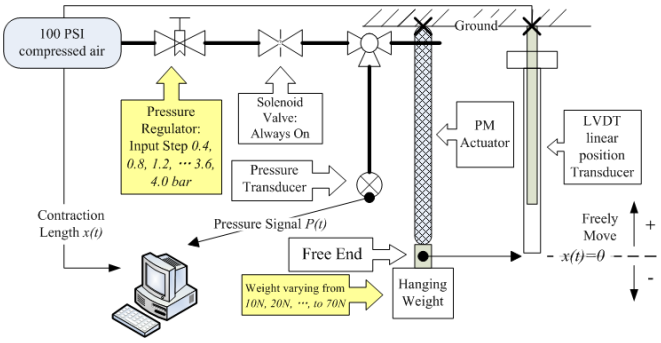

Figure 2. Schematic experimental setup

The experiment is conducted with various step pressure inputs and external loads (or weights). In each test a step pressure input is applied (solenoid valve instantly turns on) to the PM actuator. A continuous analog position signal and pressure signal are recorded in each test. Various pressure and weight values are used. The input step pressure values are changed from around the atmospheric pressure to *0.4*, *0.8*, *1.2*, *1.6*, *2.0*, *2.4*, *2.8*, *3.2* *3.6* and *4.0 bar* respectively; and loads ranged from *12.74 N* to *72.74 N* with an the increment of *10 N*, with *2.74 N* of the weight of the holder included. The purpose of using equal intervals from *0 bar* to *4 bar* is to measure the response in both lower pressure and higher pressure. Therefore, *70* tests in total have been conducted. In each test, one displacement (contraction length) response over a period of 8 seconds, and one pressure response in the same time period are recorded. An example displacement response with step input pressure of *4.0 bar* and hanging load of *20 N* is plotted in Figure 3.

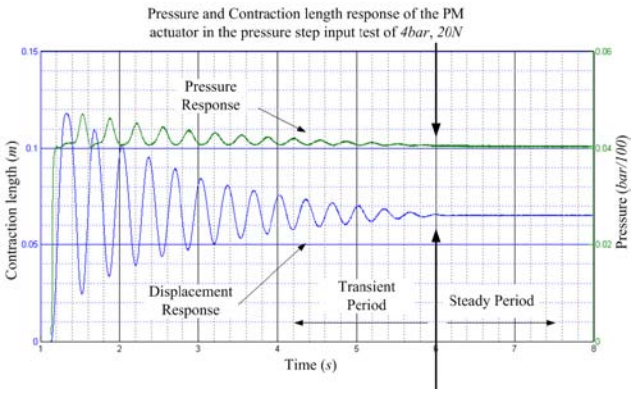

Figure 3. Sample response of the pressure step input experiment (step pressure *4 bar*, hanging weight *20 N*)

3.2 Coefficients of the Static Model

Ways of obtaining the coefficients (K_1, K_2, C_1, S_1, S_2, S_3) of the static model (Equation (3)) are varied. In order to keep their consistency in the dynamic model, the static model is determined by applying the steady state response of these tests. For example, in Figure 3, the steady-state response from *6* to *8 seconds* is used, where no damping or Coulomb friction force exists. The average values of the contraction length $x(t)$ and pressure $P(t)$ during the steady state are calculated as x_{stable} and P_{stable} respectively. Then according to the equilibrium state of the PM actuator in each step pressure input test, the static force model, Equation (3) applies and the static equilibrium is represented by the following equation of motion as:

$$\left(K_1 x^2_{stable} + K_2 x_{stable} + C_1\right) P_{stable} + S_1 x^2_{stable} + S_2 x_{stable} + S_3 - mg = 0 \quad (10)$$

The average pressure P_{stable} and average contraction length x_{stable} of each test's steady-state period are presented in Table 1 and Table 2, respectively.

Table 1: Average pressure value (in units of *bars*) during the steady-state period of each step pressure input test

Weight (N) / Pressure(bar)	12.74	22.74	32.74	42.74	52.74	62.74	72.74
0.4	0.410	0.410	0.435	0.430	0.430	0.418	0.428
0.8	0.823	0.825	0.810	0.835	0.828	0.828	0.840
1.2	1.223	1.215	1.235	1.240	1.230	1.225	1.233
1.6	1.630	1.632	1.608	1.620	/	1.595	1.593
2.0	/	2.040	2.020	2.010	2.032	2.032	2.037
2.4	2.417	2.425	2.422	2.380	2.435	2.425	2.425
2.8	2.817	2.825	2.849	2.817	2.815	2.703	2.705
3.2	3.192	/	3.232	/	3.210	3.227	3.210
3.6	3.624	3.634	3.637	3.639	3.587	3.624	3.622
4.0	4.054	4.051	4.069	3.994	4.009	3.974	4.024

Table 2: Average contraction length (in units of *mm*) during the steady-state period of each step pressure input test

Weight (N) / Pressure(bar)	12.74	22.74	32.74	42.74	52.74	62.74	72.74
0.4	1.083	1.07	0.48	0.28	-0.03	-0.06	-0.11
0.8	4.65	2.32	1.60	1.18	0.63	0.53	0.340
1.2	12.50	4.90	3.03	2.10	1.60	0.99	0.56
1.6	30.01	12.32	5.71	3.90	/	1.731	1.31
2.0	/	24.45	11.28	5.86	4.033	2.956	2.32
2.4	53.89	36.63	20.24	11.51	6.414	4.916	2.34
2.8	61.34	46.00	31.25	18.48	10.542	6.703	4.69
3.2	66.86	/	39.77	/	16.93	11.10	6.90
3.6	72.13	59.67	47.82	35.45	24.68	16.47	10.17
4.0	75.01	65.22	53.92	42.43	32.16	22.76	15.86

Multiple groups (six for the six unknown coefficients) of x_{stable} and P_{stable} data in Table 1 and Table 2 are substituted into Equation (10) to determine the coefficients. In order to prevent using data that is invalid, we tend to choose higher pressure and lower pressure cases. By using the data from the groups of (*2.8 bar*, *10 N*), (*2.0 bar*, *20 N*), (*3.6 bar*, *20 N*), (*3.6 bar*, *30 N*), (*4.0 bar*, *40 N*) and (*4.0 bar*, *50 N*) (where contraction length is in units of metres, and pressure is in the units of bar), the

following coefficients are obtained:

$$K_1 = -476.95,\ K_2 = -188.39,\ C_1 = 23.90,$$

$$S_1 = 2562.4,\ S_2 = -245.48,\ S_3 = -11.56$$

Thus the PM actuator static force model is:

$$F_{static}(x,P) = \left(-476.95x^2(t) - 188.39x(t) + 23.9\right)P(t) + 2562.4x^2(t) - 245.48x(t) - 11.56 \quad (11)$$

To verify the obtained static force model, we substitute the above contraction length and pressure values of each test stated in Table 1 and Table 2 into the static force model (Equation (3)) to provide estimation of the static force on the free end of the PM actuator. The calculation results are shown in Table 3.

Table 3: Estimated actuation force (in units of *N*) of the PM actuator in the stable period

Estimated weight (N)*& Error*	*12.74 N*	*22.74 N*	*32.74 N*	*42.74 N*	*52.74 N*	*62.74 N*
0.4 Bar	*-5.17*	*-5.18*	*-4.91*	*-5.12*	*-5.29*	*-5.59*
0.8 Bar	*5.05*	*4.60*	*4.02*	*4.41*	*4.00*	*3.95*
1.2 Bar	*12.74 (0%)*	*13.76*	*13.93*	*13.81*	*13.43*	*13.09*
1.6 Bar	*11.14 (13%)*	*21.53 (5%)*	*22.45*	*22.64*	*/*	*21.65*
2 Bar	*/*	***22.74 (0%)***	*30.21*	*31.31*	*31.81*	*31.70*
2.4 Bar	*10.98 (13%)*	*20.94 (8%)*	*33.41 (2%)*	*37.83*	*40.59*	*40.52*
2.8 Bar	***12.44 (-2%)***	*21.04 (7%)*	*32.74 (0%)*	*42.74 (0%)*	*47.59*	*46.42*
3.2 Bar	*13.16 (3%)*	*/*	*32.19 (2%)*	*/*	*51.99 (1%)*	*56.17*
3.6 Bar	*12.74 (0%)*	***22.74 (0%)***	***31.85 (3%)***	*43.08 (1%)*	*52.78 (0%)*	*60.95*
4 Bar	*12.74 (0%)*	*22.74 (0%)*	*32.74 (0%)*	***42.22 (1%)***	***53.05 (1%)***	*62.30 (1%)*

During the steady state period, the calculated static actuation forces should be very close to the hung weight on the free end of the PM actuator. The estimated force/weight results are generally in accordance with the actual hanging weight as shown in Table 3, indicating a valid static force model. It is noted that the model is only valid when the PM actuator is within its force capability limitation. The shaded background area, i.e. the upper half above the thick line in Table 3, shows the cases in which the PM actuator is beyond its force capability limitations at each pressure level. For instance, at the step input pressure level of *2.8 bar*, when the actual hung weight is applied as *12.74 N*, *22.74 N*, *32.74 N* and *42.74 N*, the estimated static forces are accurate (*12.44 N*, *21.04 N*, *32.74 N* and *42.74 N*, whose errors are *2.4%*, *7.4%*, *0.0% and 0.0%*). However, as the hanging weight increases to *52.74 N*, *62.74 N* and *72.74 N*, the estimated actuation force of the PM actuator remains at a certain value (around *46 N* to *47 N*, it slightly varies according to the actual pressure), thus failing to provide sufficient active force to lift the weights. In these cases, the PM actuator could not perform further contraction, and its length barely changes even when weights of *52.74 N*, *62.74 N* and *72.74 N* are applied. The estimation error of each estimated force within the force capability is displayed in the brackets beside the estimated forces

The estimated results in Table 3 are based on assuming the estimated weights in the cases of (*2.8 bar*, *10 N*), (*2.0 bar*, *20 N*), (*3.6 bar*, *20 N*), (*3.6 bar*, *30 N*), (*4.0 bar*, *40 N*) and (*4.0 bar*, *50 N*) equal the actual weights. These groups of force estimation results are in bold and underlined in Table 3. The rest of the estimations in this table are based on the trained static force model F_{static} from these six groups. Most of the other weight estimation results are satisfactory, with estimation error (shown in the parentheses next to each result) within *7%*. In the cases of (*2.4 bar*, *10 N*), (*1.6 bar*, *20 N*) and (*2.4 bar*, *20 N*), large misalignment is obtained (*13%*, *13%* and *8%*, respectively). These large relative error results appearing in cases of smaller weights (*10 N* and *20 N*) might be attributed to a systematic error of around *1 N* from the experiment. It becomes obvious in cases of smaller hanging weights because the estimation results are relatively small. For instance, an error value of *1 N* could lead to up to *10%* relative error in the case of *10 N* load. To exclude this error, a finer experiment should be performed in the future.

3.3 Coefficients of the Dynamic Model

After the coefficients in the static force model (K_1, K_2, C_1, S_1, S_2 and S_3) are determined and verified, the other coefficients (D_1, D_2, N_1, N_2, N_0) in the dynamic force model (Equation (9)) are also determined from the experimental data.

We used the least squares fitting approach to find the best group of coefficients (D_1, D_2, N_1, N_2, N_0). The objective function $\Psi(D_1, D_2, N_1, N_2, N_0)$ is Equation (13), in which simulation response of contraction length $x_{simu}(t)$ comes from the following equation of motion

$$m\ddot{x}(t) = F_{static} - P(t)(D_1\dot{x}^2(t) + D_2\dot{x}) - mg + \left(P(t) + \varphi(F_{ex}t)\right)\cdot\begin{cases} -\left(N_2x^2(t) + N_1x(t) + N_0\right) & (\dot{x} > 0) \\ +\left(N_2x^2(t) + N_1x(t) + N_0\right) & (\dot{x} < 0) \end{cases} \quad (12)$$

The coefficients (D_1, D_2, N_1, N_2, N_0) are estimated and adjusted until the minimum sum of the squared residual of the simulation and real contraction lengths (from the experimental results) is found, as denoted in Equation (12)

$$\Psi\left(D_1,\ D_2,\ N_1,\ N_2,\ N_0\right) = \min\left\|\sum_t \left(x_{simu}(t) - x(t)\right)^2\right\| \quad (13)$$

By using the experimental data from the valid experiments (see Table 3 for the cases that have sufficient force capability), we can obtain the optimal coefficients. In general, similar values of the coefficients are obtained from all the valid test data. Here, we presented the results obtained by using the data from the test with step pressure input of *3.6 bar* and hanging weight of *20 N* (the transient response region from *1.4* to *6 seconds*), as shown in Figure 4. The obtained dynamic force model is:

$$F(x,P) = F_{static} + \left(\ddot{x}(t) - \quad 802\dot{x}(t)\right) + \left(\frac{P(t)}{10^5} - m\right)\cdot\begin{cases} -\left(228.9342x^2(t) - 90.429x(t) + 6.87\right)(\dot{x} > 0) \\ +\left(228.9342x^2(t) - 90.429x(t) + 6.87\right)(\dot{x} < 0) \end{cases} \quad (14)$$

3.4 Model Verification and Comparison with Other Models

The obtained coefficients for each test are shown in Table 4. Accordingly, a few groups of simulation results from this model are presented in Figures 4, 5 and 6, in comparison with the experimental results.

Table 4: Optimal coefficients of (N_2, N_1, N_0, D_1, D_2) in the dynamic force model for the PM actuator in Equation (14)

(N_2, N_1, N_0, D_1, D_2)	12.74 N	22.74 N	32.74 N	42.74 N	52.74 N
1.6 Bar	224.93, -91.31, 6.86 -1.01,0.80	/	/	/	/
2 Bar	/	227.91, -90.42, 6.87, -1.01,0.80	/	/	/
2.4 Bar	228.50, -90.73, 6.87, -1.01,0.80	228.50, -90.51, 6.87, -1.01,0.80	/	/	/
2.8 Bar	228.93, -90.43, 6.87, -1.01,0.80	228.94, -90.43, 6.87, -1.01,0.80	228.95, -90.43, 6.87, -1.01,0.80	/	/
3.2 Bar	228.93, -90.43, 6.87, -1.01,0.80	/	228.93, -90.43, 6.87, -1.01,0.80	/	/
3.6 Bar	228.93, -90.42, 6.87, -1.01,0.80	228.93, -90.43, 6.87, -1.01,0.80	228.93, -90.43, 6.87, -1.01,0.80	228.94, -90.43, 6.87, -1.01,0.80	227.45, -90.43, 6.88, -1.02, 0.80
4 Bar	228.92, -90.42, 6.87, -1.01,0.80	228.92, -90.43, 6.87, -1.01,0.80	228.93, -90.43, 6.87, -1.01,0.80	228.94, -90.42, 6.88, -1.01,0.80	228.93, -90.45, 6.90, -1.01, 0.80

In Figure 4, the case of (*3.6 bar*, *10 N*) is shown. Besides the simulation results from the developed model (Equation (14)), we also applied a constant Coulomb friction force model of *2.5 N* to replace the Coulomb friction force element in Equation (14) to obtain the simulation response. The constant value of *2.5 N* is the friction value suggested by [Chou and Hannaford, 1996], in which three PM actuators of various materials that are in the same size (*11 mm* in diameter and *140 mm* long) were testsed. Since how the size affects the constant friction values was not discussed in literature, in this research, several constant friction forces (*2 N*, *2.5 N*, *4 N* and *6 N*) iare tested and compared. Similar simulation responses were obtained from the these values. Therefore, *2.5 N* is regarded as acceptable.

In this case, compared to constant friction model, better performance of the developed model is observed, especially with the varied frequency of the response.

To study this model's adaptability in handling different external loads, in Figure 5 we present the results obtained from a different experiment with a step pressure input of *3.6 bar* and load of *10 N*. In the same way the simulation results from Equation (14) and the simulation results with constant Coulomb friction are shown. It is found that, compared to the case in Figure 4, smaller external load (*10 N*) leads to higher frequence of oscillation. The constatnt Coulomb friction model (blue broken line) fails to estimate. On the other hand, the simulation from the developed model in Equation (14) is generally close to the experimental data, specifically, the frequency of simulation data agrees well with that of the experimental data well. However, it seems that the model introduces more damping compared to the experimental data.

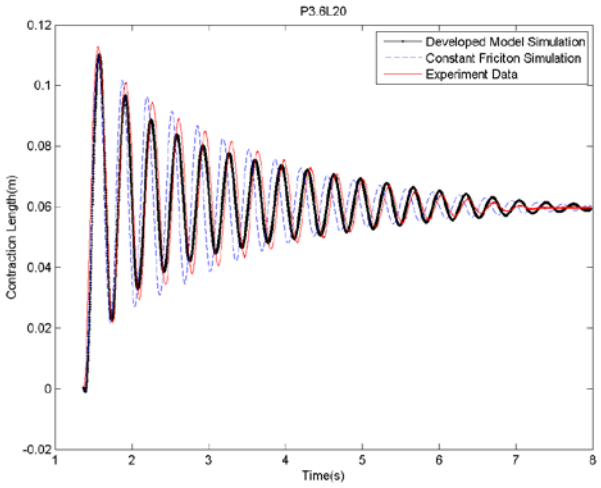

Figure 4: Comparison of results: experimental response (contraction length) with a step pressure input of *3.6 bar* and load of *20 N*; the simulation results from the case with constant Coulomb friction force of *2.5 N* suggested by [Chou and Hannaford, 1996], and the simulation data obtained by the model (Equation (14))

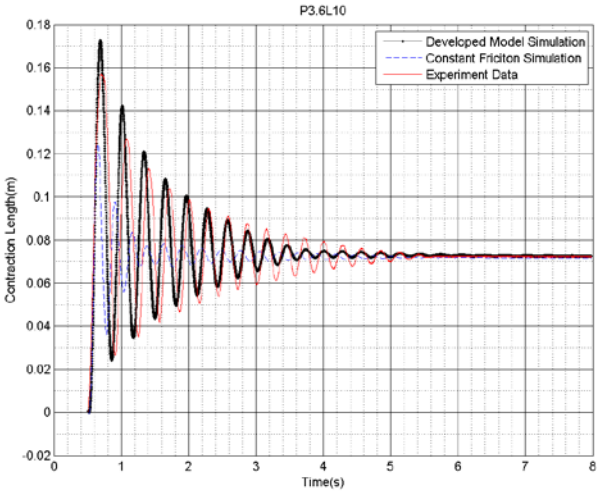

Figure 5: Comparison of results: experimental response (contraction length) with a step pressure input of *3.6 bar* and load of *10 N*; the simulation results from the case with constant Coulomb friction force of *2.5 N* suggested by [Chou and Hannaford, 1996], and the simulation data obtained by the model (Equation (14))

As for the model's performance in cases of some other step pressure levels, the case of (*2.8 bar*, *10 N*) and (*2.0 bar*, *20 N*) are displayed in Figure 6(a) and Figure 6(b) as well. Consistent performance is shown.

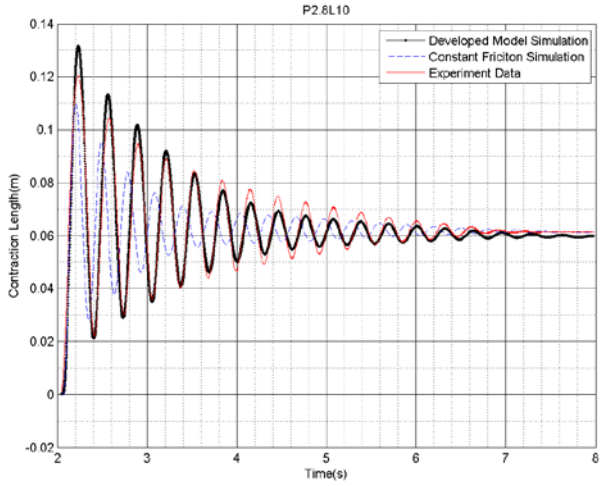

(a) Simulation and experimental results of the case of (*2.8 bar*, *10 N*)

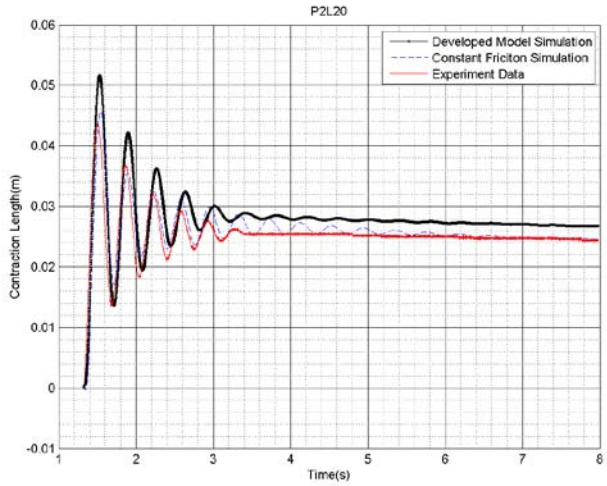

(b) Simulation and experimental results of the case of (*2.0 bar*, *20 N*)

Figure 6: Comparison of results in multiple cases: the simulation results from the case with constant Coulomb friction force of *2.5 N* suggested by [Chou and Hannaford, 1996], and the simulation data obtained by the model (Equation (14))

Compared with the simulation results in [Colbrunn et al. 2001] in Figure 7, a *6 mm* in diameter, *100 mm* long PM actuator manufactured by the same company (Shadow Robot) was tested, and the developed model also shows improvement. The PM actuator force model used in [Colbrunn et al. 2001] was assumed that the viscous damping force linearly related to the contraction velocity, and the Coulomb friction force linearly related to the PM actuator's stiffness.

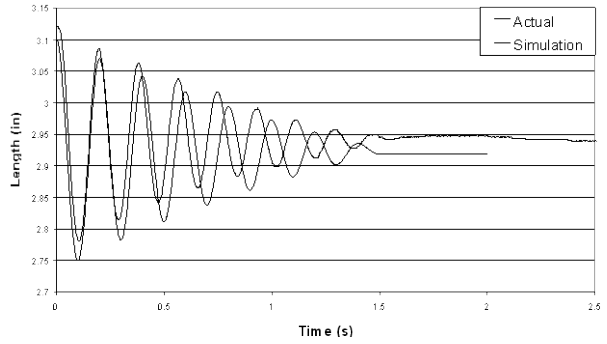

Figure 7: Comparison plot of actuator length vs. time for 60 psi nominal pressure and 6 lb suspended mass in the test in [Colbrunn et al. 2001]

Generally, the comparison of our developed dynamic model with other dynamic models is difficult because different factors relating to the PM actuator's structure, size and material can lead to different performance, as well as the way the PM actuator works. However, by comparing how different Coulomb friction models (constant or nonlinear models like the one in our model) affect the PM actuator's displacement response in the experiment of this research, as well as by studying the simula-

tion results in other researches, it is clear that our developed dynamic model has better performance with varied external loads. To the best of the author's knowledge, no other models take the external loads into account in the dynamic model. How other factors, such as the effects of creep and temperature, affect the performance of PM actuators is to be studied in the future.

4 Conclusion

In this paper, an enhanced dynamic force model for a type of small and soft McKibben-type pneumatic muscle actuator is developed. It is modelled as a high order polynomial function of contraction length, inner pressure, contraction velocity and external loads. The coefficients in this polynomial model are determined by using experimental data from experiments with different constant hanging weights and step pressure input. The coefficients are determined in two steps, in which the steady-state data are used to train the coefficients of the static force model (K_1, K_2, C_1, S_1, S_2 and S_3), and the transient response data are used for determining the coefficients of friction force elements (D_1, D_2, N_1, N_2, N_0). In the simulation studies, it is observed that the developed model yields consistently better performance over the results from the model assuming Coulomb friction as a constant force.

As part of future work, the developed model will be used in model-based control, such as the feedforward control to reduce the hysteresis.

References

[Balasubramanian et al. 2006] Sivakumar Balasubramanian, He Huang, and Jiping He, and S. Member. Quantification of Dynamic Property of Pneumatic Muscle Actuator. in *Proceedings of the 28th IEEE EMBS Annual International Conference*. pages 2734–2737. 2006

[Breteler et al, 1999] M. D. Klein Breteler, C. W. Spoor, and F. C. Van der Helm. Measuring muscle and joint geometry parameters of a shoulder for modeling purposes. *Journal of biomechanics*, vol. 32, no. 11, pp. 1191–7, Nov. 1999.

[Caldwell et al. 1995] D. G. Caldwell, Gustavo A. Medrano-Cerda, and Mike Goodwin. Control of pneumatic muscle actuators. *IEEE Control Systems Magazine*, vol. 15, no. 1, pp. 40–48, 1995.

[Chou and Hannaford, 1996] Ching-Ping Chou and Blake Hannaford. Measurement and modeling of McKibben pneumatic artificial muscles. *Robotics*, vol. 12, no. 1, pp. 90–102, 1996.

[Colbrunn et al. 2001] Robb W. Colbrunn, Gabriel M. Nelson, and Roger D. Quinn. Modeling of braided pneumatic actuators for robotic control. in *Proceedings 2001 IEEE/RSJ International Conference on Intelligent Robots and Systems*, pp. 1964–1970, 2001.

[Fei et al. 2011] Li Fei, Wang Yu, Tong Heting, and Ray P.S. Han. Empirically-Sourced Mechanical Behaviors of Pneumatic Artificial Muscles for Compensation-Based Controls. *Materials Research*, vol. 186, pp. 31–35, 2011.

[Gaylord, 1958] R.H. Gaylord. Fluid Actuated Motor System and Stroking Device. U.S. Patent 2,844,126, issued July 22, 1958

[Houghton and Carpenter, 2003] E. L. Houghton and P. W. Carpenter, *Aerodynamics for Engineering Students*. vol. 85, no. 4. Butterworth-Heinemann, 2003, pp. 500–503.

[Itto and Kogiso, 2011] Takashi Itto, and Kiminao Kogiso. Hybrid Modeling of McKibben Pneumatic Artificial Muscle Systems. in *IEEE International Conference on Industrial Technology (ICIT)*, 2011, pp. 65–70.

[Kang et al. 2009] Bong-soo Kang, Curt S. Kothera, Benjamin K. S. Woods, and Norman M. Wereley. Dynamic Modeling of McKibben Pneumatic Artificial Muscles for Antagonistic Actuation. in *IEEE International Conference on Robotics and Automation*, 2009, pp. 182–187.

[Kobayashi and Suzuki, 2005] Hiroshi Kobayashi and Hidetoshi Suzuki. A Muscle Suit for the Upper Body Development of a New Shoulder Mechanism. *IEEE Workshop on Advanced Robotics and its Social Impacts*, 2005.

[McCormick, 1995] Barnes Warnock McCormick. *Aerodynamics, aeronautics, and flight mechanics*, Wiley, 1995.

[Petrovic, 2002] P. B. Petrovic. Modeling and control of an artificial muscle part one: Model building. pages 61–68, *Trans Mech*, 47, 2002.

[Pujana-arrese et al. 2007] Aron Pujana-arrese, Ana Martinez-esnaola, and Joseba Landaluze. Modelling in Modelica of a pneumatic muscle: application to model an experimental set-up. in *21st European conference on modelling and simulation*, ECMS, 2007.

[Pytel et al. 2010]Andrew Pytel, Jaan. Kiusalaas, and Ishan Sharma, *Engineering Mechanics: Statics*, page 584, Volume 1., 3rd ed., 2010,.

[Reynolds et al. 2003] D. B. Reynolds, D. W. Repperger, C. A. Phillips, and G. Bandry. Modeling the Dynamic Characteristics of Pneumatic Muscle. *Annals of Biomedical Engineering*, vol. 31, pages 310–317, 2003

[Tondu and Lopez, 2000] Bertrand Tondu, and Pierre Lopez. Modelling and control of McKibben artificial muscle robot actuator. *IEEE Control Systems Magazine*, vol. 20, pp. 15–38, 2000.

[Wickramatunge and Leephakpreeda, 2009] K. C. Wickramatunge and T. Leephakpreeda. Empirical Modeling of Pneumatic Artificial Muscle. in *International multiconference of Engineers and Computer Scientists IMECS* , 2009, vol. II, pp. 3–7.

[Yeh et al. 2010] T.-J. Yeh, M.-J. Wu, T.-J. Lu, F.-K. Wu, and C.-R. Huang. Control of McKibben pneumatic muscles for a power-assist, lower-limb orthosis. *Mechatronics*, vol. 20, no. 6, pp. 686–697, Sep. 2010.